



OPEN

Temporal and sex-dependent gene expression patterns in a renal ischemia–reperfusion injury and recovery pig model

Stéphane Nemours¹, Luis Castro², Didac Ribatallada-Soriano¹, Maria E. Semidey³, Miguel Aranda¹, Marina Ferrer⁴, Alex Sanchez^{5,6}, Joan Morote², Gerard Cantero-Recasens¹ & Anna Meseguer^{1,7,8}✉

Men are more prone to acute kidney injury (AKI) and chronic kidney disease (CKD), progressing to end-stage renal disease (ESRD) than women. Severity and capacity to regenerate after AKI are important determinants of CKD progression, and of patient morbidity and mortality in the hospital setting. To determine sex differences during injury and recovery we have generated a female and male renal ischemia/reperfusion injury (IRI) pig model, which represents a major cause of AKI. Although no differences were found in blood urea nitrogen (BUN) and serum creatinine (SCr) levels between both sexes, females exhibited higher mononuclear infiltrates at basal and recovery, while males showed more tubular damage at injury. Global transcriptomic analyses of kidney biopsies from our IRI pig model revealed a sexual dimorphism in the temporal regulation of genes and pathways relevant for kidney injury and repair, which was also detected in human samples. Enrichment analysis of gene sets revealed five temporal and four sexual patterns governing renal IRI and recovery. Overall, this study constitutes an extensive characterization of the time and sex differences occurring during renal IRI and recovery at gene expression level and offers a template of translational value for further study of sexual dimorphism in kidney diseases.

Acute kidney injury (AKI) is a common and serious condition with no specific treatment¹ and worldwide increasing incidence². AKI is characterized by a rapid decline of renal function that requires hospital admission and renal function replacement by dialysis if renal failure is severe, leading to high mortality rates (over 50%)³. Although AKI is reversible and allows at least partial recovery of renal function, repeated AKI episodes increase the risk of subsequent chronic kidney disease (CKD) and cardiovascular disease long after recovery from the original insult^{4–8}.

Besides infection and toxic drugs, renal ischemia/reperfusion injury (IRI) is a major cause of AKI, which is faced in many clinical situations such as kidney transplantation, partial nephrectomy, renal artery angioplasty, aortic aneurysm surgery and elective urological operations⁹. In these conditions, IRI initiates a complex and interrelated sequence of events, resulting in injury and the eventual death of renal cells⁹.

Sex differences influence susceptibility, progression and response to AKI. Clinically, an increased mortality rate has been documented among males with acute renal failure^{1,10,11}. In fact, men are more prone to acute and chronic kidney disease and to progress to end-stage renal disease (ESRD) than women, when all-cause incidence rates are considered¹². Studies looking at outcomes in AKI patients have found that sex is an independent predictor of mortality^{13–15}. Consistent with clinical studies in AKI, animal research has also shown females are protected against renal IRI^{16–18}. In consequence, pre-clinical studies have been preferentially performed in males although,

¹Renal Physiopathology Group, Vall d'Hebron Research Institute, Passeig Vall d'Hebron 119-129, 08035 Barcelona, Spain. ²Biomedical Research in Urology Group, Vall d'Hebron Research Institute, Barcelona, Spain. ³Department of Pathology, Hospital Vall d'Hebron, Barcelona, Spain. ⁴Rodent Platform, Vall d'Hebron Research Institute, Universitat Autònoma de Barcelona, Barcelona, Spain. ⁵Unitat d'Estadística i Bioinformàtica, (UEB), Vall d'Hebron Research Institute, Barcelona, Spain. ⁶Department of Genetics, Microbiology and Statistics, Universitat de Barcelona, Barcelona, Spain. ⁷Departament de Bioquímica i Biologia Molecular, Unitat de Bioquímica de Medicina, Universitat Autònoma de Barcelona, Bellaterra, Spain. ⁸Red de Investigación Renal (REDINREN), Instituto Carlos III-FEDER, Madrid, Spain. ✉email: ana.meseguer@vhir.org

recently, the importance of defining pathophysiology and disease mechanisms for each sex is increasingly being integrated into biomedical research.

In this study, we have established a renal IRI and recovery model in sexually mature male and female pigs to analyze biochemical markers, histological lesions and molecular changes occurring in pre-ischemic, ischemic and post-ischemic conditions. Thorough analyses of kidney transcriptomic data were performed using Gene Set Enrichment Analysis (GSEA). Besides genes of clinical relevance, gene sets changing their expression pattern in a sex-dependent manner at different time points (basal, injury and recovery) and gene sets differentially expressed at the same time points between males and females were identified. Upon injury, changes in gene set clusters related with immune cell regulation and steroid hormone response, among others, were more prominent in males than females.

Overall, our analysis has brought novel insight into the sex-specific regulation of molecular pathways involved in IRI and recovery. Thus, this study might serve as a resource to better correlate the clinical outcome of IRI with underlying molecular processes that could eventually help to design sex-specific strategies to promote renal regeneration in humans.

Results

Renal ischemia/reperfusion injury (IRI) pig model reveals sex-dependent structural and functional renal changes. In order to study the changes in gene expression occurring after ischemia/reperfusion injury (IRI), we proceeded to generate an IRI model in sexually mature pigs. Previous studies on the effects of warm ischemia^{19–24} reported that periods greater than 30 min can lead to severe kidney damage and periods longer than 60 min irreversible damage. Thereby, ischemic kidney injury was induced in single-kidney female and male pigs by clamping the renal pedicle for 30 min and data was obtained before the surgery (PR), five minutes after ischemia (PS) and one week later (WL) (schematized in Fig. 1A). To confirm our kidney injury–recovery pig model, blood urea nitrogen (BUN) and serum creatinine (SCr) were measured at basal situation before injury (PR), at 5 min post-reperfusion (PS) and at 24 h (1d), 72 h (3d) and one-week (WL) post-reperfusion (Fig. 1B). In pigs, normal SCr values range from 0.6 to 1.6 mg/dL, which is in accordance with the values found in our study (1.14 mg/dL for both males and females). Regarding BUN, normal levels in pigs range from 10 to 30 mg/dL, which fits with our basal values as well (18 mg/dL and 15 mg/dL for males and females, respectively). The increment in SCr and BUN levels was statistically significant 24 h after ischemia compared to normal basal values for both males and females (SCr = 2.97 mg/dL and 3.36 mg/dL, respectively; BUN = 55 mg/dL and 58 mg/dL, respectively). Then values gradually descended at 3 and 7 days post-surgery for sexes without reaching those at PR, which indicates that the recovery process was still ongoing (Supplementary Table 1). For the scope of this study, we focused on three time points (PR, PS and WL) for subsequent analyses.

No significant differences were detected between males and females regarding SCr and BUN parameters at any time point (Fig. 1B). The fact that sex differences have been well documented in the incidence, the severity and the mortality in AKI events in human and animal models, provides more relevance to our findings once proved that SCr and BUN levels lack sex-specificity.

Kidney histopathological examination at PR, PS and WL showed near-normal renal morphology with changes associated with sublethal injury including mild interstitial edema and mononuclear infiltration as well as tubular injury associated to brush border diminishment^{25–27} (Fig. 1C). To assess if there was any difference between males and females, we quantified tubular damage (Jablonski scoring system (SS)²⁸) and interstitial mononuclear infiltration. Our data revealed that tubular damage was more prominent in males than females (Levels 2–3 of Jablonski SS: 40% of males at PS and 20% at WL vs. 0% of females at PS and WL) (Fig. 1D upper panel). On the contrary, mononuclear infiltrates (level 1) were more common in females at PR (40% females vs. 0% males), reached similar incidence for both sexes at PS (80% in both males and females) and remained present in 60% of the females but not in males at WL (Fig. 1D lower panel). Altogether, females present more mononuclear infiltrates than males, both at pre-surgery and at one-week after reperfusion, while males exhibit more tubular injury than females at PS and WL. Importantly, according to biochemical and histological parameters, our data indicate that recovery is still ongoing at 7 days post-reperfusion in both sexes.

Kidney transcriptome profiles across injury and recovery in female and male pig samples. Next, in order to identify the time- and sex-dependent molecular pathways relevant for IRI and recovery, we performed a microarray-based gene expression analysis using samples from our IRI pig model. To investigate major changes in the transcriptional response before, during and after IRI, we performed a hierarchical clustering of gene expression levels, represented as heatmaps that allowed the identification of common and distinct patterns of regulation between different experimental conditions. In both males and females, time point comparison revealed a similar gene expression pattern between pre-ischemia (PR) and post-ischemia (PS), which was radically different one week later (WL) (Fig. 2A). Interestingly, sex comparison results indicate that changes in global gene expression observed at PR and PS between males and females disappear during the recovery phase (WL) (Fig. 2B), with males exhibiting a global female-like phenotype during recovery.

Validation of microarray data by qRT-PCR. In order to assess the reliability of the microarray data, selected genes changing their expression in a time and sex-dependent manner (*IFIT3*, *FABP5*, *CXCI0*, *CD274*, *RSAD2*) (Fig. 3A) were analyzed by qRT-PCR using specific TaqMan probes. Our data show that these genes chosen for the validation presented a similar pattern as in the microarrays, therefore confirming the trustworthiness of the microarray data (Fig. 3B).

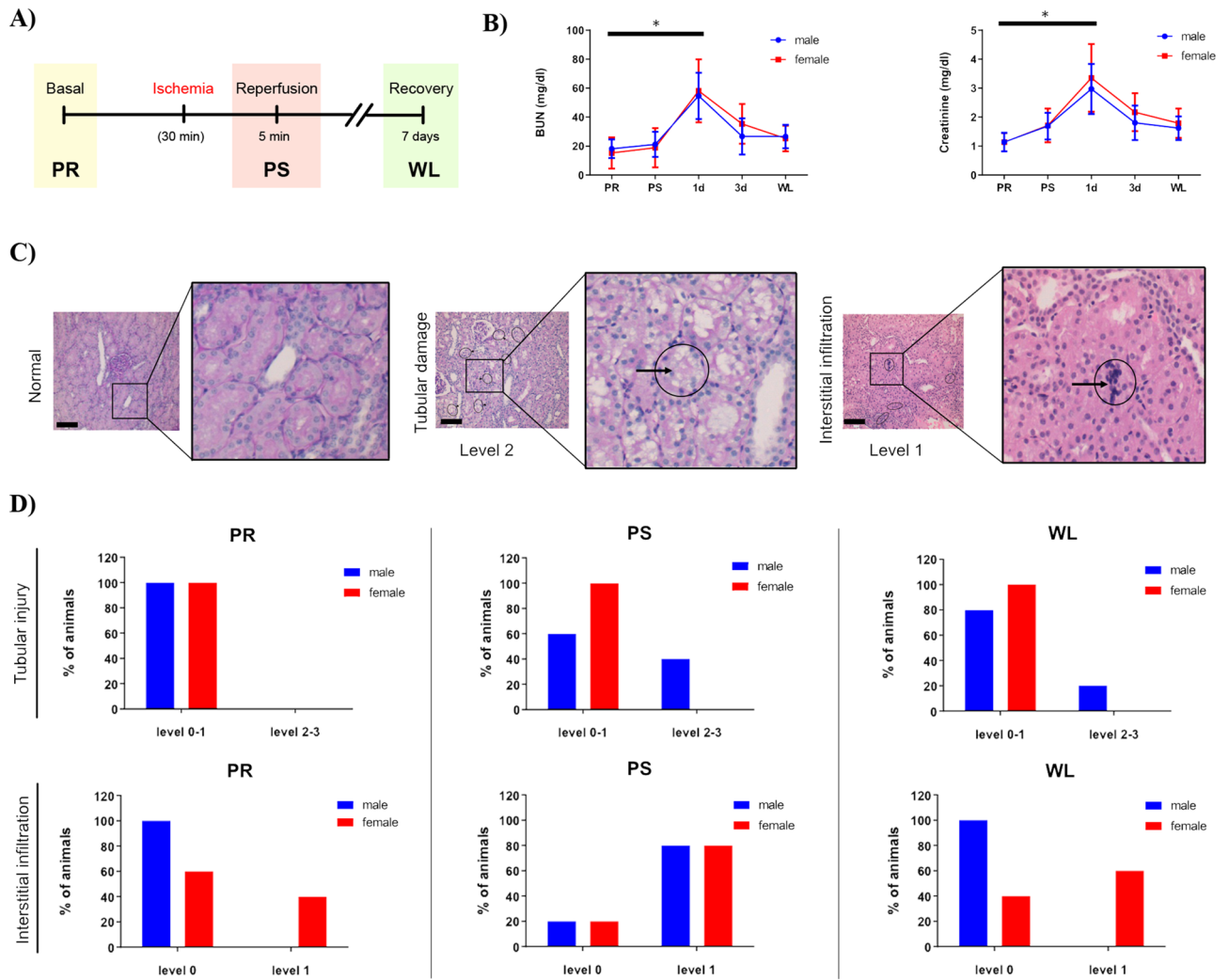


Figure 1. Assessment of biochemical parameters and histological examination following porcine renal ischemia/reperfusion injury. **(A)** Experimental design of renal unilateral IRI following contralateral nephrectomy. Ischemia was induced for 30 min. Data were collected before injury, 5 min and 7 days following renal clamping. **(B)** Measurement of blood urea nitrogen (BUN) and serum creatinine (SCr) levels in males (blue) and females (red). The “y” axis represents blood urea nitrogen and serum creatinine concentration, respectively, and the “x” axis represents the time points. Average values \pm SEM are plotted in the graph (N = 5). **(C)** Representative images of different levels of tubular injury and interstitial infiltration in pig kidney. Arrows indicate specifically damaged cells. Magnification = 20X, scale bar = 100 μ m. **(D)** Quantification of tubular injury (upper panel) and interstitial infiltration (lower panel) scored by an expert pathologist was classified by group and sex (males in blue, females in red). The y-axis represents the % of animals showing each level of injury or infiltration, respectively. BUN blood urea nitrogen, PR pre-ischemia, PS post-ischemia, WL one week later. * $p < 0.05$.

mRNA levels of pig-selected genes relevant for IRI are conserved in humans. In order to study the conservation of the gene expression pattern in humans, selected genes showing sex-dependent regulation by renal ischemia in pigs (i.e., *IFIT3*, *FABP5*, *CXCL10*, *CD274*, *RSAD2*) were analyzed in ischemic kidney biopsies from men and women. Briefly, kidney biopsies of normal tissue were obtained from renal cancer patients of both sexes undergoing nephrectomy. There were no significant differences in terms of patients’ clinical indexes relative to cardiovascular or renal pathology between both sexes (Supplementary table 11). Non-tumoral post-ischemic tissues were collected after 30 min of ischemia, approximately, thus corresponding to the post-surgery (PS) condition in our pig model. Next, we tested the mRNA levels of the selected genes in these post-ischemic kidneys of men and women by quantitative PCR (qRT-PCR). Importantly, from the five genes analyzed, *RSAD2*, *CXCL10* and *CD274* showed the same expression pattern observed in the pig model (*RSAD2*: men: 0.8462 ± 0.1322 , women: 0.5015 ± 0.1036 ; *CXCL10*: men: 0.7169 ± 0.1500 , women: 0.4909 ± 0.0917 ; *CD274*: men: 1.219 ± 0.1505 , women: 0.7965 ± 0.0608), while no differences were detected for *FABP5* or *IFIT3* between sexes (Fig. 3C). Overall, a partial correlation was found between the mRNA levels of both species, under ischemic conditions.

Together, our data suggest that *RSAD2*, *CXCL10* and *CD274* might serve as noninvasive surrogated biomarkers to predict ischemic injury and recovery in human kidneys.

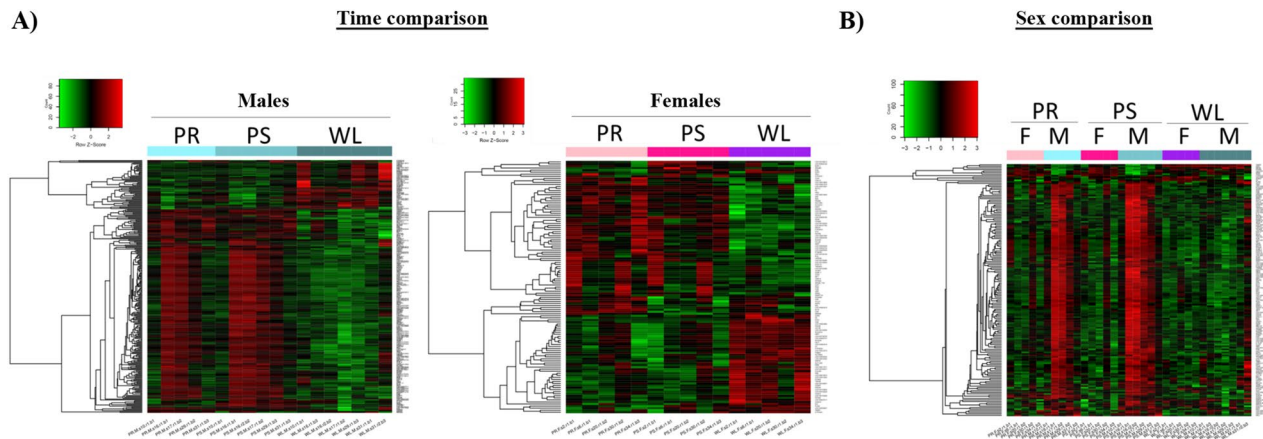


Figure 2. Hierarchical clustering of microarray assays based of kidney porcine throughout renal IRI in a time and sex manner. Gene expression for males and females were compared at different time points (PR, PS, and WL). **(A)** Heatmaps graphically illustrating the differences in the gene expression levels for the time comparison in males (left) and females (right). Similar pattern of expression was observed for both sexes. **(B)** Heatmap representing the difference in expression by comparing males and females at the same time point (sex comparison). The green color represents genes with lower expression and the red color represent the ones with higher expression. Genes represented in the heatmaps have an adj. p value ≤ 0.25 and $|\log FC| \geq 1$. *F* female, *M* male, *PR* pre-ischemia, *PS* post-ischemia, *WL* one week later.

Time comparison reveals differentially expressed genes throughout renal IRI. We have analyzed those transcripts altered throughout IRI (up- and down-regulated) to identify common and exclusive genes for each time point (PR, PS, WL). In males, 174 genes were conserved between the WL versus PR and WL versus PS comparisons, 52 genes were exclusive of WL versus PS comparison and 50 genes were only found in the WL versus PR comparison. From the eight genes that are different between PS and PR, only two (*LEAP2*, *MIR505*) are exclusive of this comparison (Fig. 4A). Our results revealed similar patterns for each comparison in females, although lesser genes were altered compared to males. Specifically, 59 genes were conserved between the WL versus PR and WL versus PS comparisons, 19 genes were exclusive of WL versus PS comparison and 37 genes were only found in the WL versus PR comparison (Fig. 4B). Interestingly, one gene (*FOS*) was shared between the WL versus PR and the PS versus PR comparisons. Finally, from the eight genes differentially expressed between PS and PR, four are specific for this comparison (*NKL*, *KLF5*, *DNAJB1* and *CPE*).

Altogether, our data suggest that renal injury and recovery processes have a lower impact in females than males. The overall number of differentially expressed genes in renal IRI and recovery in male and female pig kidneys are reported in the supplementary Fig. 1 (adj. p value ≤ 0.25 , without considering the fold change, supplementary Fig. 1).

Sex comparison of gene expression during renal injury and repair. Fifty-one of the 53 differentially expressed genes between sexes at basal (PR) remained unchanged after injury (PS), while 109 genes changed in males during this phase (Fig. 4C). It is very relevant to state that all gene expression changes found between males and females at PR and PS disappeared at WL and only two genes, *SLC51A* and *DHRS7*, were differentially expressed between sexes in this phase. The number of differentially expressed genes throughout renal IRI and recovery between males and females at the same time point are reported in supplementary Fig. 2 (adj. p value ≤ 0.25 without considering the fold change, supplementary Fig. 2).

Role of androgens in the regulation of differentially expressed genes (DEG) during IRI. The aim of this study was to identify differences between male and females pig kidneys that could be of translational value for men and women. Our results showed a clear difference in gene expression between both sexes during the IRI and the recovery process, thus we postulated that sexual hormones might have a role. Since androgens have been related with worst outcome in experimental models and patients, we compared the gene expression profile of the top DEG between male and female pigs over IRI with data from a single castrated male (CM) using the Ingenuity Pathways Analysis (IPA) software. The reasons to use a single CM is because pig castration has become a social and ethical issue. Therefore, taking into account the aim of the study, we considered that one single CM would be sufficient as a proof of concept to prove the androgenic control of certain genes in pig kidney.

Interestingly, the CM sample, which was not included in the enrichment pathway analyses, phenocopies the gene expression pattern of females at basal conditions (PR) (Fig. 5A). Moreover, the CM does not completely follow the gene expression pattern of males at PR and WL (Fig. 5B). Specifically, genes that follow a putative androgen-dependent expression in PR (i.e., *UBD*, *IFIT3*, *CXCL11*, *FBG*, *FGG*, *MX1*, *IFIT1* and *CXCL10*) show an opposite direction at WL between males and CM. On the other hand, those that are common between males and CM (i.e., *CKAP2*, *CENPF*, *CDC20*, *KIF20A*, *CCNA2*, *EPHB3*, *C6*, *SLC6A19* and *FABP5*) in PR, retain the same pattern of expression at WL. These results suggest that androgens and male sexual hormones may contribute to the sexual dimorphic expression pattern observed at basal conditions, in renal injury and during recovery.

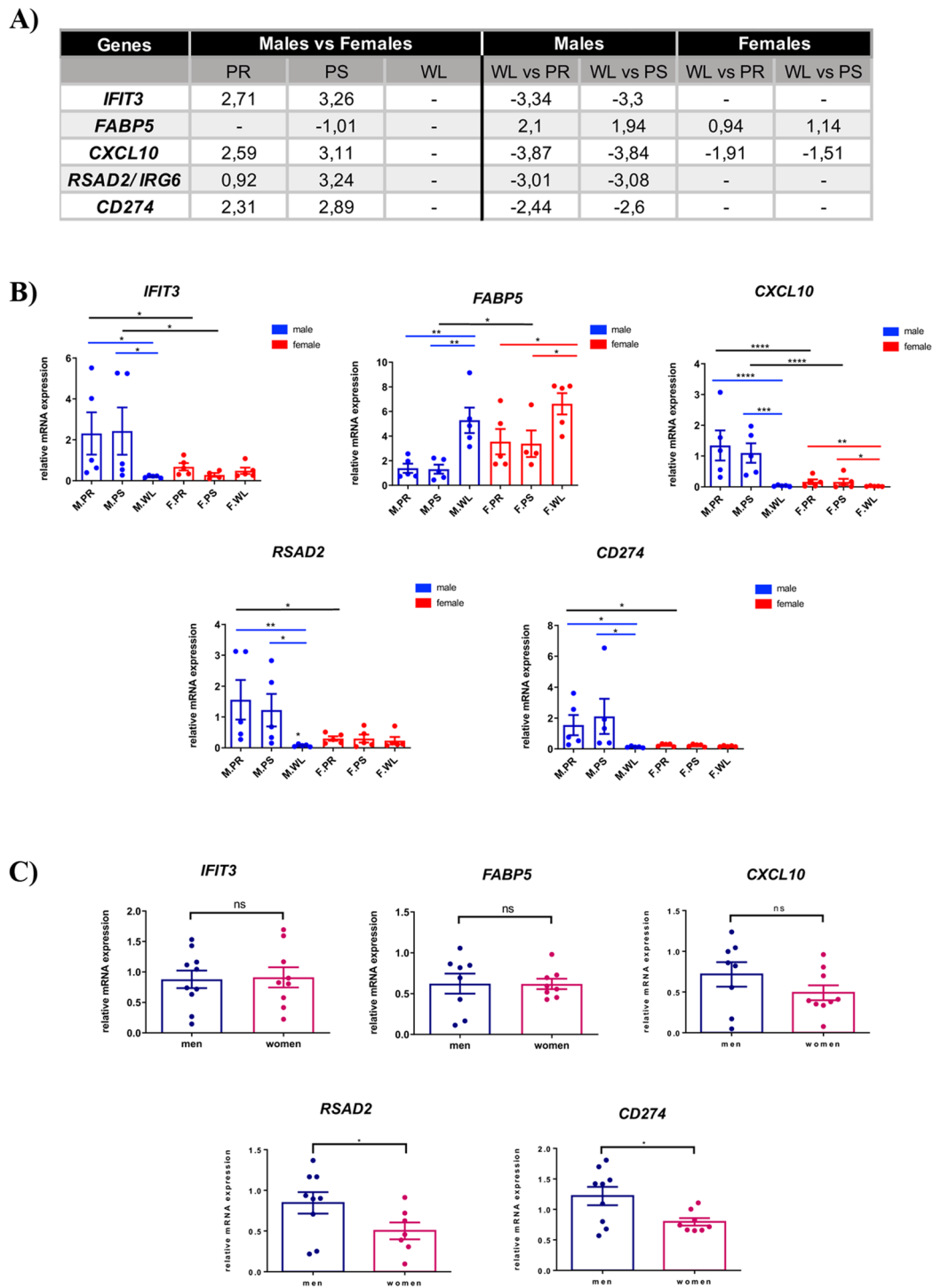


Figure 3. Validation of porcine renal IRI microarray assays by qRT-PCR experiments followed by evaluation of mRNA levels of selected targets in human ischemic kidney biopsies. **(A)** Expression values of five selected targets from microarray assays displaying time and sex differences. **(B)** Relative mRNA levels of *FABP5*, *IFIT3*, *RSAD2*, *CXCL10*, *CD274* were measured and compared by qRT-PCR. For the time comparison, the different time points (PR, PS, WL) were compared with each other for each sex (blue male, red female). For the sex comparison, a selected time point in male was compared to the equivalent time point in female. Blue and red lines represent a time comparison in male or female, respectively. Black lines represent sex comparison at equivalent time points. **(C)** *RSAD2*, *CXCL10*, *CD274*, *FABP5* and *IFIT3* expression levels were evaluated by qPCR in post-surgery (PS) conditions from samples of 36–80 and 53–83 years old men and women, respectively (N > 7). **p* value ≤ 0.05; ***p* value ≤ 0.01; ****p* value ≤ 0.001; *****p* value ≤ 0.0001, ns: not significant. *F* female, *M* male, *PR* pre-ischemia, *PS* post-ischemia, *WL* one week later.

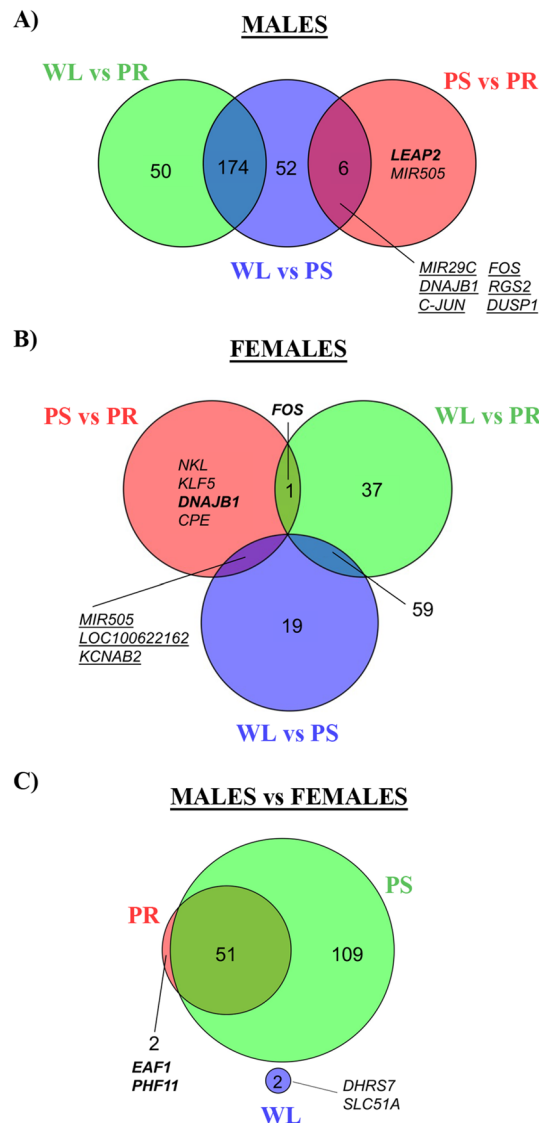


Figure 4. Venn diagrams of time and sex comparisons between males and females throughout renal IRI. Venn diagrams depicting the number of commonly regulated genes (A) in male and (B) in females at different time point comparisons: PS versus PR, WL versus PS and WL versus PR. Males showed an overall higher number of regulated genes. (C) Venn diagrams depicting the number of commonly regulated genes in the sex comparison at different time points: PR, PS and WL. Only two genes were commonly regulated one week following injury. Genes represented only in italic are down-regulated, whereas genes in bold and italic are up-regulated. Genes underlined are both up- and down-regulated in respective comparisons. Complete gene tables are available in supplemental material. adj. p value ≤ 0.25 and $\log |FC| \geq 1$. F female, M male, PR pre-ischemia, PS post-ischemia, WL one week later.

Gene Set Enrichment Analysis (GSEA) reveals the importance of immune system related pathways during the recovery process in males. Our study has identified differentially expressed genes (DEG) between female and male pig kidneys at basal conditions (PR), injury (PS) and recovery (WL). To gain mechanistic insight into time- and sex-related differences that govern renal injury and recovery processes, we aimed to identify which biological pathways are differentially expressed between groups using Gene Set Enrichment Analysis (GSEA).

As an example of the GSEA, here we show the comparison between males and females at one-week post reperfusion (M.WL vs. F.WL). For this particular comparison, the GSEA showed that over-represented clusters (in red) in males include: regulation and production of cytokines and interleukins, immune somatic recombination, microtubule cytoskeleton organization, actin organization and mitotic cycle transition. On the other hand, under-represented clusters (in blue) contain nodes related with metabolism of fatty acids and steroid hormones, nucleotide biosynthetic processes, amino acid catabolism and response to xenobiotic stimulus, amongst others (Fig. 6A). Moreover, deeper analysis of each of these nodes led to specific gene sets. For instance, the somatic

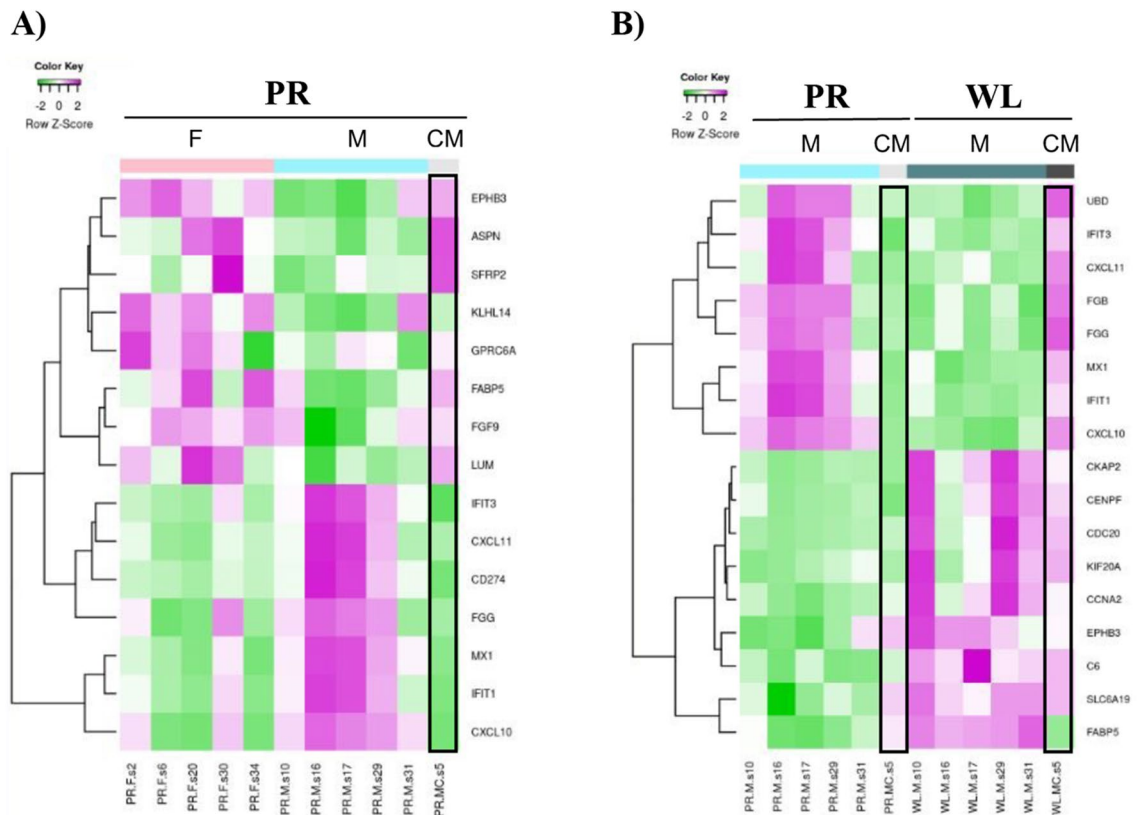


Figure 5. IPA heatmap gene expression representation of top regulated genes. Microarray data files of pig experiments were uploaded in IPA software. Results were reported in hierarchical clustering of top up and down regulated genes in (A) a sex- (M vs F) and (B) time- (M vs WL) comparisons. Data from a castrated male was compared with male and female pig expression patterns. The castrated male showed a gene expression pattern similar to females. *F* female, *M* male, *CM* castrated male, *PR* pre-ischemia, *WL* one week later.

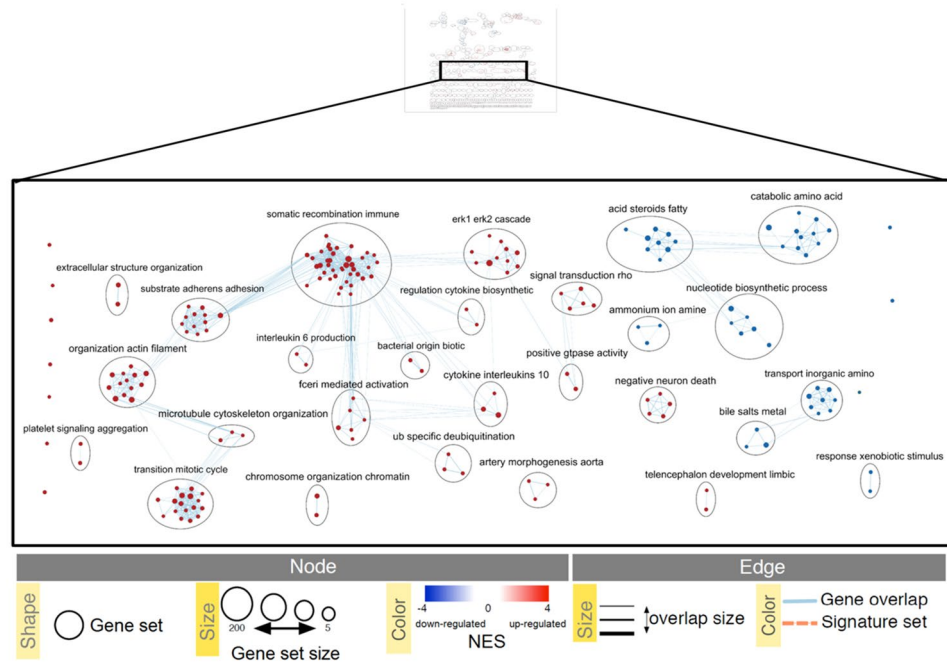
recombination immune node (up-regulated) includes gene sets like lymphocyte activation or B-cell differentiation; while the down-regulated node of fatty acids and steroid hormones includes metabolism of steroids or metabolism of lipids (Fig. 6B). We performed the same analysis for the other sex and time comparison before, after injury and during recovery. The lists of 10 top up- and down-regulated gene sets enriched for each comparison are reported in the supplementary tables 2–10. Overall, our results revealed the sex-specific regulation of gene sets upon IRI.

Grouped enrichment analyses of sex and time comparisons show the gene sets controlling renal injury and recovery.

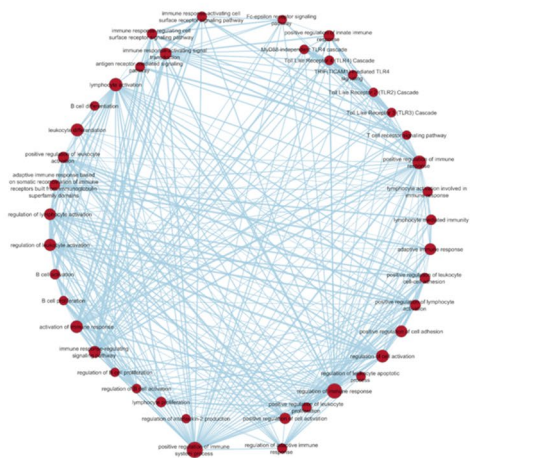
Besides individual comparisons and to get insight into the overall processes, we performed grouped comparison visualization of the enrichment analyses. Heatmaps including the six time comparisons (F.PS vs. F.PR; F.WL vs. F.PR; M.PS vs. M.PR; M.WL vs. M.PR; M.WL vs. M.PR) or the 3 sex comparisons (M.PR vs. F.PR, M.PS vs. F.PS, M.WL vs. F.WL) were created. The addition of multiple comparisons in a single enrichment map hindered an effective visualization of gene sets involved in chosen clusters. Nine clusters containing high numbers of gene sets, which revealed their prominence in the processes under study, were selected from the enrichment maps. The NES (normalized enrichment score) value of each of the gene sets included in the nine clusters were indicated in heatmaps. The nine clusters are: (I) immune cell regulation, (II) morphogenesis development migration, (III) ion transport transmembrane, (IV) apoptotic intrinsic extrinsic, (V) oxygen levels hypoxia, (VI) alcohol biosynthetic process, (VII) steroid hormone response, (VIII) regulation hormone secretion and (IX) phagocytosis endocytosis and invagination. Interestingly, the regulation of gene sets of a distinct cluster varies amongst different comparisons (examples in Figs. 7A and 8A).

Grouped GSEA analyses reveal different temporal gene set regulation patterns after renal IRI and recovery. Heatmaps representing gene sets of previously selected clusters (for instance, the Immune cell regulation cluster shown in Fig. 7A) allowed the visualization of five prominent temporal patterns of expression that are schematically represented in Fig. 7B. To simplify our analysis, we focused on gene sets that are over-regulated, assuming that this leads to higher activity of those genes involved in IRI events. Importantly, gene sets from the nine clusters can follow different or similar temporal patterns revealing coordinated expression (Fig. 7B and Tables 1, 2, 3, 4, 5). The five temporal patterns that we have identified are (Fig. 7C):

A) Sex comparison: Male WL vs Females WL



B) Immune Somatic Recombination node



Fatty acids and steroids node



Figure 6. Enrichment map example of over-represented genes in individual sex comparisons M.WL versus F.WL following GSEA analyses. **(A)** Representation of different clusters (nodes) regulated in the comparison. The map allows visualization of clusters containing nodes in which red and blue represent up- or down-regulated gene sets for each node, respectively. The clusters take their name from the most common containing names of the nodes within the cluster. **(B)** Example of the different gene sets that form somatic recombination immune and acid steroids fatty nodes, where red and blue nodes represent up- or down-regulated gene sets, respectively (FDR: 0.01–0.1).

1. *Pattern 1* includes gene set clusters that are over-represented during the recovery process in females (WL vs. PS) and in the injury process in males (PS vs. PR) (see Table 1 for complete gene sets included in pattern 1).
2. *Pattern 2* is composed of pathways over-represented during the recovery process (WL vs. PS) in females but never found in males (Table 2).
3. *Pattern 3* includes gene sets that are only over-represented in males during injury (PS vs. PR) (Table 3).
4. *Pattern 4* is composed of gene sets over-represented during the recovery process (WL vs. PS) and at one-week post-reperfusion (WL vs. PR) in females; and also over-represented only during injury in males (PS vs. PR) (Table 4).
5. *Pattern 5* involves pathways that are over-represented only during injury in both sexes (PS vs. PR) (Table 5).

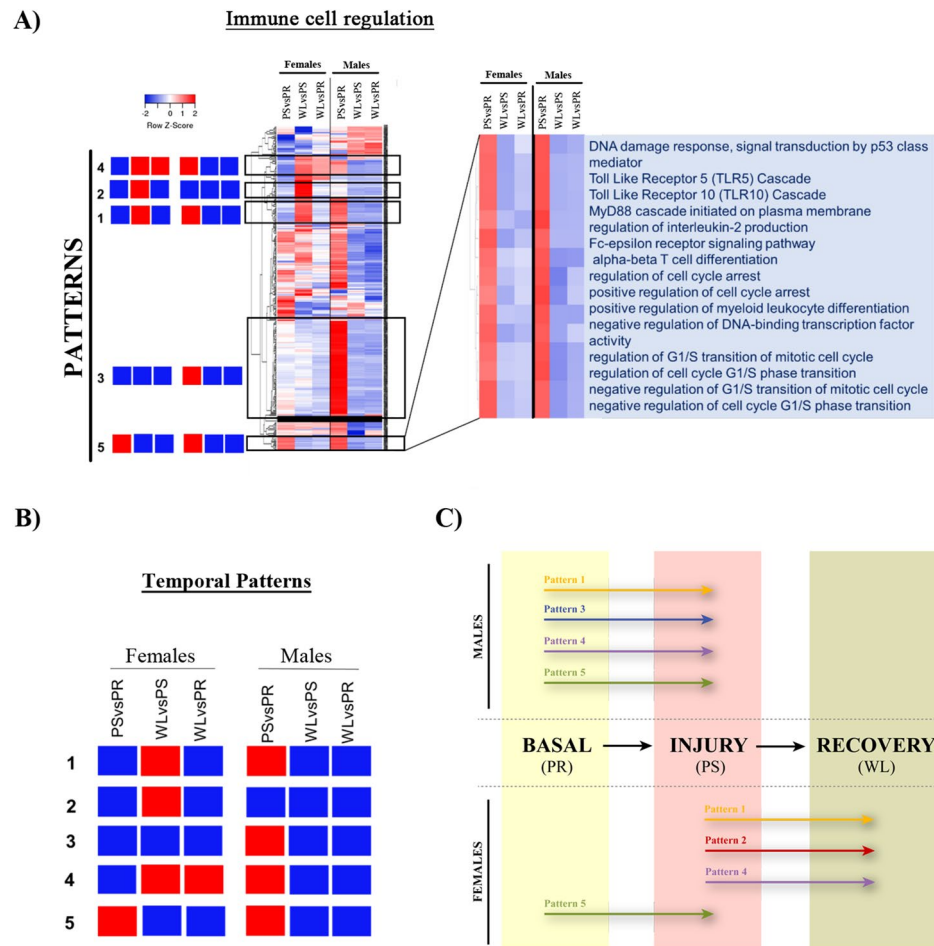


Figure 7. Patterns of gene sets regulation in male and female kidneys throughout renal IRI in the time comparison. An example of the gene sets of selected clusters represented by hierarchical clustering. **(A)** Heatmap (of time comparisons) was created with the normalized enrichment score (NES) values of the gene sets calculated by GSEA analysis. The red and blue colors refer to gene sets that are over- or under-represented in the heat-maps. **(B)** Five prominent patterns for time comparison were determined. **(C)** A summary of these five temporal patterns is depicted in a diagram, where patterns displayed in each sex are illustrated by a colored arrow positioned at the time point where they are up-regulated (PR, PS, WL). PR pre-ischemia, PS post-ischemia, WL one week later.

GSEA analyses reveal four sex-dependent gene set regulation patterns. Finally, we have created heatmaps for the sex comparison (for example, for the immune cell regulation cluster shown in Fig. 8A), which revealed four prominent sex-dependent patterns (from A to D) schematically shown in Fig. 8B. We performed the same type of analysis as for time comparison to regroup the gene sets and clusters that shared similar expression pattern (Tables 6, 7, 8, 9) (Fig. 8C).

- *Pattern A* includes gene sets that are up-regulated in males versus females both at basal conditions (PR) and after injury (PS) (Table 6).
- *Pattern B* includes over-represented gene sets in males at injury (PS) (Table 7).
- *Pattern C* includes pathways over-represented in males at injury (PS) and after one-week reperfusion (WL) (Table 8).
- *Pattern D* is followed by pathways over-activated in males one week after reperfusion (Table 9).

Discussion

Ischemia is the most common etiology for acute kidney injury (AKI) and one of the main contributors to morbidity and mortality in the hospital setting, as it affects 1 out of 5 patients in emergency admissions²⁹. Experimental studies have also shown that AKI is associated with mild-to-moderate acute injury in organs distant from the kidney such as the liver, lung or brain therefore precipitating or aggravating other conditions that may have

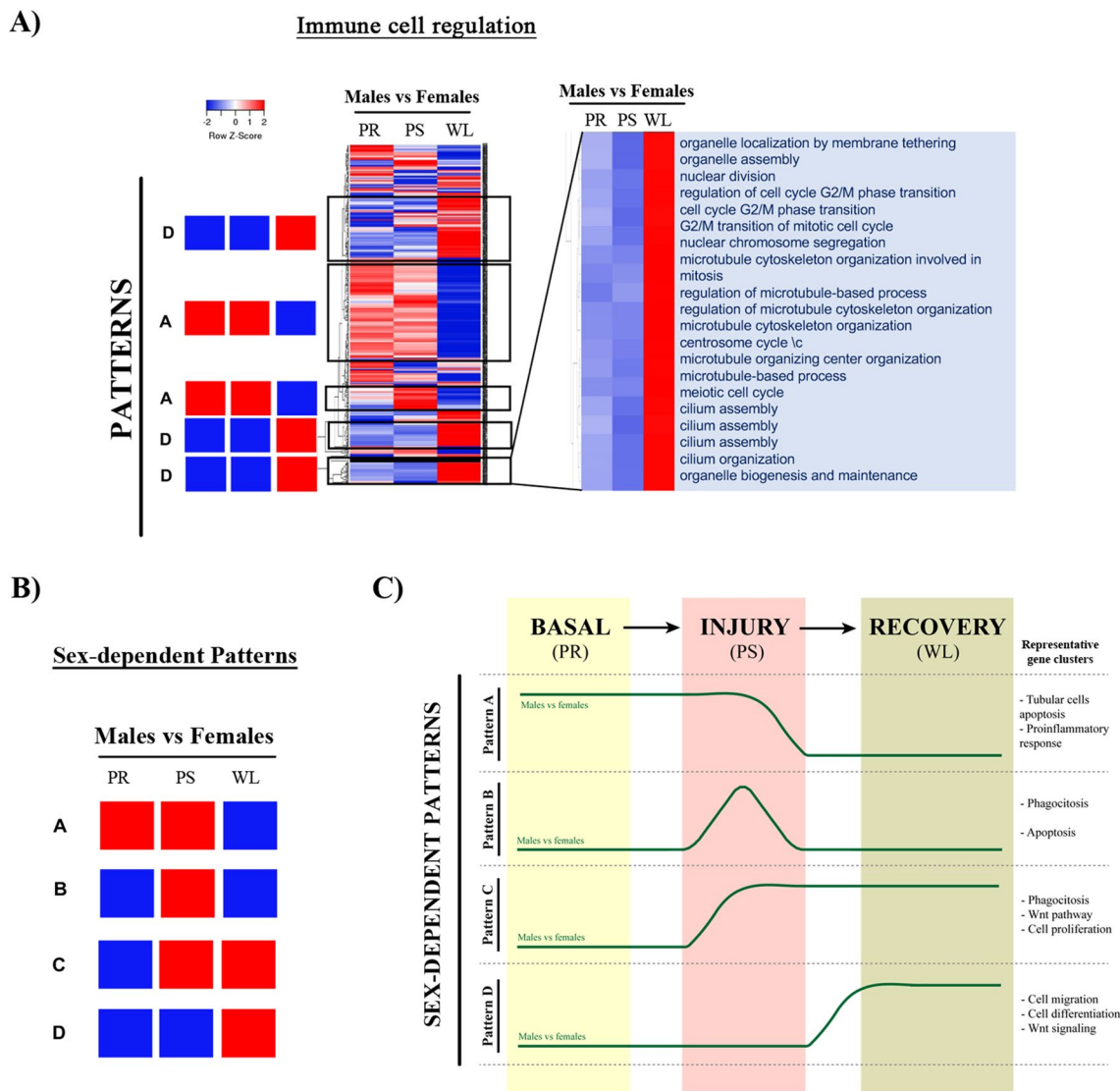


Figure 8. Patterns of gene sets regulation in male and female kidneys throughout renal IRI in the sex comparison. Gene sets of selected clusters were represented by hierarchical clustering. **(A)** Heatmaps (of sex comparisons) were created with the normalized enrichment score (NES) values of the gene sets calculated by GSEA analysis. The red and blue colors refer to gene sets that are over- or under-represented in the heat-maps. **(B)** Four prominent patterns for sex comparison were determined. **(C)** A summary of these four temporal patterns is depicted in a diagram. *PR* pre-ischemia, *PS* post-ischemia, *WL* one week later.

significant impact on patients' morbidity and life expectancy³⁰. The initiating insult might be irreversible but, in many cases, timely intervention to restore renal perfusion may mitigate the severity of evolving ischemic AKI, by preventing still functioning tissue from progressing to overt injury. AKI occurrence also displays sex differences, men being generally more prone to suffer from AKI, to progress more frequently to chronic kidney disease (CKD) and to end stage-renal disease (ESRD)³¹.

Novel renal Ischemia/Reperfusion Injury (IRI) pig model. Pigs represent the gold standard model for renal transplantation research and studies involving IRI in tubule interstitial fibrosis development. Pigs present advantages over other animal models because their similarities with humans (e.g. genome, size, metabolism and renal anatomy)^{32–35}, being some biochemical parameters identical (e.g. SCr and BUN)^{24,25,36}. Importantly, the size of their kidney allows sample collection at different time points from same animal, overcoming the individual variability and disparity that might occur in rodents. Moreover, as indicated in the Materials and Methods section, samples were comparable since we took the same amount of tissue from the same part of the kidney for all animals. This is an extremely privileged situation for the study of sex- and temporal- dependent structural, biochemical and molecular events occurring in kidney injury/regeneration processes, in a model that is the closest possible to humans. Additionally, data collection from a porcine model has a significant advantage over data coming from clinical reports since the former can pinpoint and clearly define ischemia-related events versus other concomitant factors that may occur in patients.







	Female			Male		
	PSvsPR	WLvsPS	WLvsPR	PSvsPR	WLvsPS	WLvsPR
Pattern 1						
I-Immune cell regulation	Myeloid cell differentiation					
	Negative regulation of cell cycle					
	Regulation of alpha-beta T cell activation					
	Positive regulation of T cell activation and differentiation					
	Positive regulation of cell-cell adhesion					
II-Morphogenesis development migration	Positive regulation of mononuclear cell migration					
	Regulation of leukocyte migration					
	Positive regulation of leukocyte chemotaxis					
III-Ion transport transmembrane	Calcium regulation, concentration and transport					
	Negative regulation of phosphate metabolic process					
VI-Alcohol biosynthetic process	Regulation of cholesterol metabolic process					
	Alcohol biosynthetic process					
	Steroid biosynthetic process					
	Steroid metabolic process					
VII-Steroid hormone response	Lipid metabolism					
	Response to organonitrogen compound					
IX-Phagocytosis endocytosis invagination	Phagocytosis, engulfment					
	Regulation of endocytosis					
	Regulation of vesicle-mediated transport					
	Endocytosis					

Table 1. Summary of clusters and gene sets included in the pattern 1 for the renal IRI time comparison.







	Female			Male		
	PSvsPR	WLvsPS	WLvsPR	PSvsPR	WLvsPS	WLvsPR
Pattern 2						
I-Immune cell regulation	Inflammatory response					
	Increase TNF production					
	Necrotic cell death					
	Humoral immune response					
	Positive regulation of adaptive immune response					
II-Morphogenesis development migration	Negative regulation of blood vessel morphogenesis					
	Negative regulation of angiogenesis					
	Negative regulation of epithelial cell proliferation					
IX-Phagocytosis endocytosis invagination	Positive regulation of endocytosis					
	Membrane invagination					
	Receptor metabolic process					

Table 2. Summary of clusters and gene sets included in the pattern 2 for the renal IRI time comparison.







	Female			Male		
	PSvsPR	WLvsPS	WLvsPR	PSvsPR	WLvsPS	WLvsPR
Pattern 3						
I-Immune cell regulation	T cell proliferation and activation					
	Regulation of leukocyte cell–cell adhesion					
	Regulation of mononuclear cell proliferation					
	Toll-Like receptors cascades					
	MyD88 cascade TLR4 TRIF					
II-Morphogenesis development migration	Biomineral tissue development					
	Positive regulation of endothelial cell migration					
	Regulation of smooth muscle cell migration					
	Bone mineralization					
	Retina development					
	Regulation of cell motility					
	EMT					
III-Ion transport transmembrane	Regulation of ion transmembrane transporter activity					
	Phosphorylation					
	Fatty acid transport					
IV-Apoptotic intrinsic extrinsic	Negative regulation of extrinsic apoptotic signaling pathway					
V-Oxygen levels hypoxia	Response to decreased oxygen levels					
	Cellular response to hypoxia					
VII-Steroid hormone response	Cellular response to lipid					
	Cellular response to insulin					
	Cellular response to hormone					
VIII-Regulation hormone secretion	Positive regulation of hormone secretion					
	Protein transport					
	Protein localization					
	Cytokine secretion					

Table 3. Summary of clusters and gene sets included in the pattern 3 for the renal IRI time comparison.

Our IRI pig model presents the highest SCr and BUN values, markers of renal injury, at 24 h post-reperfusion in both males and females. Their levels gradually descend and remain slightly elevated seven days after injury, which indicates an ongoing recovery process. This reproduces the course of ischemic AKI observed in patients, where the process from insult to first evidence of recovery takes between 7 and 21 days²⁹. Although both sexes showed similar levels of SCr and BUN, kidney histopathological examination revealed sublethal injury with higher mononuclear infiltrates in females than males. These data correlate with the immune response sexual dimorphic pattern observed in humans^{37,38}. On the other hand, tubular injury associated to brush border diminishment was still present in males at 7 days post-injury. This indicates that the renal recovery after IRI is delayed in males compared to females, suggesting a role for sexual hormones in this process.

Identification of sexual dimorphism in the time-specific gene expression controlling renal IRI and recovery. The first key result of this IRI pig model is that males exhibit stronger global gene expression changes during injury and recovery than females. It is striking the opposite expression pattern observed in males compared to females even at basal (PR) or during injury (PS), which is completely reversed with males acquiring a female-like gene expression pattern at 7 days post-surgery (WL). Altogether, these data point to a clear role for the sexual hormones in the protection against IRI and recovery after renal injury. Only two genes (*SLC51A* and *DHRS7*) remain differentially expressed at 7-day post-surgery between males and females. *DHRS7* encodes for the seventh member of the short-chain dehydrogenases/reductases (SDR) family, which metabolize many different compounds, including steroid hormones³⁹. *SLC51A* encodes the alpha subunit of the organic solute transporter alpha/beta (*OSTα/β*), which is a heteromeric solute carrier protein that transports bile acids, steroid metabolites and drugs into and out of cells⁴⁰. The differential regulation between sexes of genes that metabolize and transport sex steroid hormones during recovery suggests a link between their expression and renal repair after injury.

Amongst the genes with differential expression between females and males at basal conditions or during injury, but exhibiting similar levels during recovery, the ones with the highest differences are those related with







	Female			Male		
	PSvsPR	WLvsPS	WLvsPR	PSvsPR	WLvsPS	WLvsPR
Pattern 4						
I-Immune cell regulation	Neutrophil degranulation					
	Neutrophil activation					
	Neutrophil mediated immunity					
	Granulocyte activation					
	Myeloid cell activation					
	Leukocyte degranulation					
	Humoral immune response mediated by circulating immunoglobulin					
III-Ion transport transmembrane	Negative regulation of ion transmembrane transport					
	Negative regulation of cation transmembrane transport					
VI-Alcohol biosynthetic process	Metabolism of steroids					
	Organic acid biosynthetic process					
	Regulation of lipid biosynthetic process					
	Cholesterol biosynthetic process					
VII-Steroid hormone response	Response to organophosphorus					
	Response to organic cyclic compound					
	Response to estradiol					

Table 4. Summary of clusters and gene sets included in the pattern 4 for the renal IRI time comparison.







	Female			Male		
	PSvsPR	WLvsPS	WLvsPR	PSvsPR	WLvsPS	WLvsPR
Pattern 5						
I-Immune cell regulation	α - β T cell activation					
	DNA damage response					
	TLR5/TLR10					
	MyD88 cascade					
	IL-2					
	Regulation of cell cycle arrest					
III-Ion transport transmembrane	Negative regulation of ERK1 and ERK2 cascade					
	Negative regulation of MAP kinase activity					
VIII-Regulation hormone secretion	Positive regulation of secretion of hormone metabolism processes					
	Hormone secretion					
	Protein transport					
	Protein localization					
	Cytokine secretion					

Table 5. Summary of clusters and gene sets included in the pattern 5 for the renal IRI time comparison.

immune and inflammatory processes. For example, interferon signaling pathways related genes (*MX1*, *IFIT3* and *GBP1*), interferon responding genes (*CXCL9*, *CXCL10* and *CXCL11*), programmed cell death 1 ligand 1 (*PDL1/CD274*), inflammatory response protein 6 (*IRG6/RSAD2*) and a protease that cleaves complement components *C2* and *C4* (*MASP2*)⁴¹. All these genes are strongly and significantly overexpressed in males compared


Male vs Female	
PR PS WL	
	
Pattern A	
I-Immune cell regulation	Leucocyte cell–cell adhesion
	T cell differentiation and activation in immune response
	TNF production
	INF γ production
	NF- κ B signaling
	Toll-like receptor signaling pathway (TLR3/TLR4)
	Complement cascade
II-Morphogenesis development migration	Positive regulation of leucocyte chemotaxis and migration
	Cellular response to chemokine
	Positive regulation of mononuclear cell migration
III-Ion transport transmembrane	Cytosolic calcium
	Calcium transport
	Positive regulation of cytosolic calcium ion concentration
IV-Apoptotic intrinsic extrinsic	Intrinsic apoptotic signaling pathway
	Intrinsic apoptotic signaling pathway by p53 class mediator
	Regulation of signal transcription by p53
VI-Alcohol biosynthetic process	Steroid biosynthetic process
	Regulation of cholesterol biosynthesis by SREBP (SREBF)
	Metabolism of steroids
	Lipid biosynthesis and metabolism
	Inositol phosphate metabolic process
	Cellular ketone metabolic process
VII-Steroid hormone response	Cellular response to hormone stimulus
	Peptide
	Estradiol
	Cellular response to insulin stimulus (insulin receptor signaling pathway)
VIII-Regulation hormone secretion	Regulation of peptide, protein, hormone secretion and transport by cell

Table 6. Summary of clusters and gene sets included in the pattern A for the renal IRI sex comparison.

to females at basal conditions or right after injury, with no differences at seven-days post-injury indicating that they acquire a female-like expression phenotype.

Nevertheless, albeit presenting similar expression of immune related genes at recovery, the histopathological analysis shows higher mononuclear infiltrate in females. A possible explanation is that same ligands can have different effects depending on the cell type. For instance, chemokines CXCL9, CXCL10 and CXCL11 are ligands of the CXCR3 receptor and play important roles in the activation and stimulation of the immune system against foreign antigens⁴². However, CXCR3 positive T regulatory (Treg) cells infiltration are beneficial for proper kidney allograft function⁴³. This dual effect could explain why females are more protected against IRI than males. One of the limitations of our study has been the poor performance of available antibodies to detect pig proteins by WB and IHQ assays, thus enabling us to correlate differential gene expression with immune cell infiltrates in kidney tissues.

Role of sexual hormones in the regulation of IRI and renal recovery controlling genes. Our data showed that the expression pattern of putative sex-regulated genes in the castrated male was closer to females than males, confirming the impact of male sexual hormones on IRI and recovery. This is the case, for example, for *FABP5*, *CD274*, *IFIT3* and *CXCL10* genes, likely indicating the androgen-dependent regulation of their expression. In fact, *FABP5* has been found to be a potential therapeutic target in prostate cancer, an androgen-dependent cancer type⁴⁴. Moreover, androgens have been shown to up-regulate *CXCL10* expression in prostate epithelial cells⁴⁵.

Comparison between humans and pigs data: PDL1 as a candidate. An important part of our study was to prove the correlation between pigs and humans, so our discoveries could be used to treat renal IRI.




Male vs Female	
<div style="display: flex; justify-content: space-around; align-items: center;"> <div style="text-align: center;">PR </div> <div style="text-align: center;">PS </div> <div style="text-align: center;">WL </div> </div>	
III-Ion transport transmembrane	Inorganic cation transport and homeostasis
	Potassium ion transport
	Striated muscle contraction
	Amino acid transport
IV-Apoptotic intrinsic extrinsic	Negative regulation of intrinsic apoptotic signaling pathway
V-Oxygen levels hypoxia	Cellular response to hypoxia
VI-Alcohol biosynthetic process	Cholesterol metabolic process
	Steroid metabolic process
	Regulation of fatty acid metabolic process
VII-Steroid hormone response	Cellular response to organonitrogen compound

Table 7. Summary of clusters and gene sets included in the pattern D for the renal IRI sex comparison.




Male vs Female	
<div style="display: flex; justify-content: space-around; align-items: center;"> <div style="text-align: center;">PR </div> <div style="text-align: center;">PS </div> <div style="text-align: center;">WL </div> </div>	
II-Morphogenesis development migration	Positive regulation of epithelial cell proliferation
	Eye morphogenesis
	Positive regulation of endothelial cell proliferation
	Positive regulation of Wnt signaling pathway
IX-Phagocytosis endocytosis invagination	Internalization
	Engulfment
	Import into cell
	Receptor-mediated endocytosis

Table 8. Summary of clusters and gene sets included in the pattern C for the renal IRI sex comparison.

Our data from human samples show that the expression levels of *CXCL10*, *RSAD2* and *CD274* (PDL1) are lower in females than males, similar to what was observed in our pig model. Amongst them, *CD274/PDL1* is one of the most interesting candidates. This protein is a ligand of PD-1, a negative co-stimulatory molecule expressed by T lymphocytes, monocytes, dendritic cells, and B cells⁴⁶. The interaction between PD-1 and PDL1, present on antigen-presenting cells and tumor cells, constitutes an immune checkpoint through which tumors can induce T-cell tolerance and avoid immune destruction⁴⁶. It appears that PDL1 on non-immune cells participates in Treg-mediated protection against kidney IRI and AKI⁴⁷. However, further research is required to study how PDL1 lower levels in females can protect them against injury.

Time and sex-dependent IRI and repair pathways. Besides individual genes, our -omics data allowed the identification of clusters containing gene sets relevant for processes associated with renal IRI and recovery, providing evidence of their sex- and temporal-regulated fashion.

Sex and time comparison of gene sets of most prominent clusters. Here we have identified five temporal patterns for different gene clusters and four sex-dependent patterns. The behavior of these temporal and sex-dependent patterns is summarized in Figs. 7C and 8C. First, early after IRI (PR to PS), genes following *pattern 5* are activated in both males and females, but males also specifically activate the genes following *pattern 3*. Interestingly, *pattern 1* and *pattern 4* include genes expressed after injury in males, but one week later (recovery) in females. Finally, the *pattern 2* is specific for females one week after the injury. In order to understand the meaning of this




Male vs Female	
<div style="display: flex; justify-content: space-around; align-items: center;"> <div style="text-align: center;">PR </div> <div style="text-align: center;">PS </div> <div style="text-align: center;">WL </div> </div>	
Pattern D	
I-Immune cell regulation	IL6-6/IL-2
	TLR 5/10
	DNA damage checkpoint
	Cell cycle checkpoint
	Mast cell activation
	Humoral immune response
	Mitotic DNA integrity checkpoint
	Negative regulation of G1/S transition
	B cell proliferation and activation
	TLR1, TLR2 cascade, TLR6
	Cell-substrate adherens
Cell-matrix adhesion	
II-Morphogenesis development migration	Angiogenesis
	Blood vessel morphogenesis
	Endothelial cell migration and proliferation
	Canonical Wnt signaling pathway /non-canonical Wnt signaling pathway
	Kidney development
	Mesonephric epithelium development and tubular development
IX-Phagocytosis endocytosis invagination	Morphogenesis of a polarized epithelium
	Positive regulation of endocytosis
	Phagocytosis
	Receptor metabolic process
	Regulation of vesicle-mediated transport

Table 9. Summary of clusters and gene sets included in the pattern B for the renal IRI sex comparison.

temporal and sex-dependent regulation, as well as the clusters activated at each time point, we propose the following:

In the *early phases of renal IRI*, reduced oxygen supply to metabolically active tubular epithelial cells lowers oxidative metabolism and depletes cell supplies of high-energy phosphate compounds. Reperfusion restores the oxygen supply, which results in mitochondrial impairment, enhances oxygen free radicals formation and, therefore, causes more injury⁴⁸. Interestingly, males and females react differently to this situation. Males activate gene sets in response to a decrease in oxygen levels and hypoxia (*Pattern 3*), while females show negative regulation of angiogenesis during the recovery phase (*Pattern 2*). Altogether, our data likely indicate that males suffer more from the lack of oxygen than females.

Tubular epithelial cell apoptosis is the key pathophysiological alteration occurring in IRI, and defines the extent of the damage to kidney function⁴⁸. This process mainly occurs through the intrinsic pathway⁴⁹ by p53, which is highly activated in males at both basal and injury conditions (*Pattern A*), suggesting that males are preferentially affected by apoptotic damage. This fits well with the histopathological results showing more tubular injury associated to brush border diminishment in males than females. Androgens are known to inhibit apoptosis and promote growth^{50,51}. However, upon cellular stress, they can also promote stress-mediated apoptosis by enhancing mitochondrial translocation of the proapoptotic protein Bax, which plays a critical role in the intrinsic apoptotic pathway via mitochondrial membrane permeabilization⁵².

Another process leading to tubular epithelial cell death is *necrosis*. Necrotic cell death is accompanied by the release of immunogenic cellular components collectively known as damage-associated molecular patterns (DAMPs), which cause severe tissue damage, leading to systemic inflammation⁵³. Apoptosis and regulated necrosis can occur at the same time in the same kidney compartment, as they are not mutually exclusive and coexist in many renal pathological conditions⁴⁸. Gene sets related with necrotic cell death are upregulated in females during recovery (*Pattern 2*), occurring later than apoptosis in males. Interestingly, our results point to sex hormones as a relevant factor pushing towards apoptosis or necrosis in front of the same trigger and intensity event.

During IRI, both sexes activate gene sets related with DNA damage, the innate immune response, T cell activation, cytokine secretion and cell cycle arrest, which are downregulated during recovery (*Pattern 5*). Together with tubular epithelial cells, macrophages produce proinflammatory cytokines, thus contributing to injury. Gene

sets and clusters controlling these pathways are preferentially upregulated in males (*Pattern 3*). Besides, males also present enhanced activation of pro-inflammatory pathways (e.g., *TNF alpha* and *IFN γ* production, *NFKB* signaling and complement cascade) not only during injury but also at basal situation (*Pattern A*). Concomitantly, negative regulation of MAP kinase activity and positive regulation of hormone metabolism processes also occur in both sexes, contributing to the reestablishment of cellular homeostasis.

Although the *immune response* has an important role during these processes for both sexes, gene sets involved on immune cell regulation, mononuclear cell migration, leukocyte chemotaxis, phagocytosis and engulfment are activated at different time points in males and females. Genes following *patterns 1* and *4* are active at injury in males but enhanced in females during recovery, which correlates with the apoptotic and necrotic events occurring in males and females at these time points, respectively. Our histology data also revealed higher mononuclear infiltrates in females at recovery, which is in agreement with gene sets following *pattern 2* (upregulated in females during recovery) controlling inflammatory response, TNF alpha production, humoral response and adaptive immune responses. These processes are even clearer when we compare male and female at the same time points, which reveals that genes related to phagocytosis are more activated in males at injury and during recovery (*Pattern C* and *Pattern D*).

The renal tubular epithelium has a huge capacity for *regeneration after injury*. During the repair process, surviving tubular cells actively proliferate and differentiate into mature tubular cells to reconstruct their functional structures. Regeneration of the tubular system is essential for recovery from AKI and a clear marker of patient morbidity⁴⁸. The clinical end-point of abnormal repair is chronic kidney disease that is reflected, histologically, by tubular atrophy and renal fibrosis due to myofibroblast proliferation and deposition of extra-cellular matrix²⁹. Regeneration involves actions of endogenous inhibitors of inflammation, up-regulation of repair genes, actions of the immune system, clearance of necrotic and apoptotic cells and tubular regeneration²⁹. Gene sets regulating these pro-regenerative processes through the immune system are activated one week after the injury in our model, especially in females (*Pattern 4*). We also observed that gene sets related to extra-cellular matrix and cellular migration are upregulated in males during injury (*Pattern 3*), which indicates an effort to replace lost cells to repair the tubular system, a phenomenon that usually occurs within less than a week⁴⁸.

As shown by gene sets included in *Pattern C*, males show a positive regulation of Wnt signaling pathway, endocytosis and engulfment at injury and during recovery, likely reflecting that injury has a stronger effect in males. It is also apparent a negative regulation of the intrinsic apoptotic pathway during injury (*Pattern B*) possibly due to the induction of EMT (epithelial-mesenchymal transition) in males (*Pattern 3*). The EMT activation together with increased epithelial and endothelial cell proliferation that occurs in males during injury and recovery (*Pattern C*) might allow males to recover from the ischemic insult. Moreover, the migratory capacity provided by EMT enables these transitional cells to invade the basement membrane and repopulate the injured tubules⁵⁴. *Pattern D* shows that males at recovery exhibit augmented transcriptional programs related with endothelial cell migration and differentiation, kidney development, morphogenesis and epithelium recovery, associated to the activation of canonical and non-canonical Wnt signaling. Activation of Wnt/ β -catenin seems to be instrumental for tubular repair and regeneration after AKI, recapitulating the role of Wnt signaling in kidney embryonic development⁵⁵.

Conclusions

Our results show that sex hormone have an impact on the type of gene sets regulated in the kidney during IRI and recovery and also on the timing of their activity. Steroid biosynthesis, hormone secretion and hormones transport are up-regulated in males compared to females in basal conditions and after injury. These differences are abolished one-week after injury, fitting with the feminized gene expression pattern shown by males during recovery, which might likely represent a survival mechanism to diminish androgen promotion of stress-mediated apoptosis. Altogether, our study provides a template to further characterize renal IRI in a temporal and sex specific manner that might bring us one step closer to the development of effective treatment strategies for kidney diseases in the human population.

Materials and methods

Animals. This study was conducted using farm pigs, hybrids between Large White and Landrace. Five females, five males and one castrated male of four months old, free of specific pathogens, between 30 and 40 kg of weight were included in this study. This age range was chosen due to the sexual maturity of the animal, allowing hormone effects. Regarding the number of animals per group, we follow the three Rs principle (Reduce, Replace, Refine) in our experimental design. In addition, there are several ethical issues to be considered when using pigs as experimental model⁵⁶. Finally, the fact that we can take samples from the same animals at different time points, reduces variability, therefore requiring a lower number of animals per group. All animal experiments complied with the ARRIVE guidelines. All animal care and procedures were performed in accordance with the requirements of the European laws on the protection of animals used for scientific and experimental purposes (86/609 EEC), and has the approval by the Experimental Ethics Committee of the Vall d'Hebron Institute of Research (VHIR) (34/08 EAEC).

Experimental design. On the first day of surgery, expert urology surgeons from the team practiced a laparoscopic left nephrectomy followed by 30 min of warm ischemia in the right kidney. The left kidney was defined as control tissue at basal state (PR), clear from injury. By performing a left nephrectomy, the compensation of the other kidney to maintain renal function during ischemia–reperfusion injury was prevented. Upon ischemia, the lower pole of the kidney was removed (approximately 3 cm of kidney parenchyma) and after suturing, and 5 more minutes of arterial reperfusion, an upper polar biopsy was obtained (approximately 1 cm of renal parenchyma). Animals were housed until day 7-post surgery, when a laparoscopic nephrectomy of the right

kidney was performed. Pigs were then euthanized at that point. Overall, three kidney biopsies were collected for each animal: prior to injury (PR), 5 min following 30 min of ischemia (PS) and one week after ischemia (WL) (Fig. 1A). In addition to tissues, blood samples were collected at the different time points of the experiment including 1 and 3 days following ischemia.

Assessment of renal injury by serum analysis. Creatinine and urea serum levels were analyzed on blood samples obtained through the cannulation of the carotid artery and the internal jugular vein (placed during the first surgery). The catheters subcutaneously tunneled were kept until the end of the experiment for each animal. The determination of serum creatinine was performed by the buffered kinetic reaction of Jaffe (diagnostic system of Boehringer Mannheim) with a Roche / Hitachi 917 system. Serum urea determination was performed by extracting 3 ml of blood with heparin to extract plasma (GD kinetic UV, Human, No. 10521). Measures were taken with a Cobas Mira Plus[®] 6 autoanalyzer and a Hitachi 4020[®] spectrophotometer.

Assessment of renal injury by histological examination. All animals underwent baseline renal biopsies followed by subsequent biopsies just after ischemia and one-week after injury. Samples were prepared by 10% formalin fixation and paraffin embedding, followed by staining with hematoxylin and eosin and Periodic acid–Schiff. A blinded pathologist using standard light microscopy assessed the degree of lesions at the tubular and interstitial level of all biopsy samples. The epithelial tubular affection was scored as follow: 0: absence or dilation with reduction of the brush border; 1: proximal vacuolization with some isolated necrotic cell; 2: proximal vacuolization with disseminated necrotic cells; 3: proximal vacuolization with groups of necrotic cells. The Interstitial affection was score thereby: 0: absence of inflammatory infiltrate or < 10% of parenchyma; 1: inflammatory infiltrate 10–25% of the parenchyma; 2: Inflammatory infiltrate 25–50% of the parenchyma; 3: Inflammatory infiltrate > 50% of the parenchyma.

Microarray experiment. RNA was extracted from the PR, PS and WL kidney biopsies from each animal. The extractions were performed starting from 50 mg of each biopsy performed with the NZyol Kit following manufacturer instructions (Nzytech genes & enzymes). Microarray hybridization was carried out at High Technology Unit (UAT) at VHIR. RNA integrity was assessed by Agilent 2100 Bioanalyzer (Agilent, Palo Alto, Ca). Only samples with similar RNA integrity number were accepted for microarray analysis. Gene Titan Affymetrix microarray platform and the Genechip Porcine Gene 2.1 ST 16-Array plate were used for this experiment. This array analyzes gene expression patterns on a whole-genome scale on a single array with probes covering many exons on the target genome, and thus permitting expression summarization at the exon level or gene level. Starting material was 200 ng of total RNA of each sample. Briefly, sense ssDNA suitable for labeling was generated from total RNA with the GeneChip WT Plus Reagent Kit from Affymetrix (Affymetrix, Santa Clara, CA) according to the manufacturer's instructions. Sense ssDNA was fragmented, labeled and hybridized to the arrays with the GeneChip WT Terminal Labeling and Hybridization Kit from the same manufacturer.

Microarray data analysis. All microarray data in this publication have been deposited in NCBI's Gene Expression Omnibus^{57,58} and are accessible through GEO Series accession number GSEXXXXX (<http://www.ncbi.nlm.nih.gov/geo/query/acc.cgi?acc=GSEXXXXX>). Bioinformatic analysis was performed at the Statistics and Bioinformatics Unit (UEB) at VHIR. Robust Multi-array Average (RMA) algorithm⁵⁹ was used for pre-processing microarray data. Background adjustment, normalization and summarization of raw core probe expression values were defined so that the exon level values were averaged to yield one expression value per gene. The analysis was done considering the experimental factors (time points and sex) and taking into account the pairing between samples in most of the comparisons performed. Data were subjected to non-specific filtering to remove low signal and low variability genes. Conservative thresholds were used to reduce possible false negative results. This yields a list of 3435 genes to be analyzed. Selection of differentially expressed genes was based on a linear model analysis with empirical Bayes modification for the variance estimates⁶⁰. This method is similar to using a 't-test' with an improved estimate of the variance. To account for multiple testing, *p* values were adjusted to obtain stronger control over the false discovery rate (FDR), as described by the Benjamini and Hochberg method⁶¹. Genes with adjusted *p* value below 0.05 and absolute value of log₂ fold change over 1 were called differentially expressed.

Quantitative Reverse-transcription polymerase chain reaction (qRT-PCR). Microarray experiments were validated by qRT-PCR experiments. Up to 2 µg of total RNA was retro-transcribed using the High-Capacity RNA-to-cDNA Master Mix (Applied Biosystems) and used to perform quantitative gene expression analyses using TaqMan[®] Gene Expression Master Mix (Applied Biosystems). qPCR was performed in a 7900HT Fast Real Time PCR system (Applied Biosystems, Inc.). These specific TaqMan probes were used: *IFIT3* (Ss04248506_s1); *FABP5* (Ss03392150_m1); *CXCL10* (Ss03391845_g1); *CD274* (Ss03391947_m1) and *RSAD2* (Ss03381589_u1). To confirm the use of equal amounts of RNA in each reaction, all samples were examined in parallel for beta-actin (Ss03376160_u1). Triplicate PCR amplifications were performed for each sample. mRNA levels of human ischemic kidney biopsies were also measured at the same conditions. Non-tumoral post-ischemic renal tissues from 10 men and 9 women (36–83 years old) undergoing nephrectomy for renal cancer treatment were collected after 30 min of ischemia, thus corresponding to the post-surgery (PS) condition in our pig model. Description of patient's relevant clinical indexes, especially those which may affect kidney (cardiovascular pathology, diabetes and renal pathology, mainly) is included in supplementary table 11 (Supplementary table 11).

None of the patients had undergone chemotherapy or immunotherapy before nephrectomy. Specific TaqMan probes were used: *IFIT3* (Hs01922752_s1); *FABP5* (Hs02339439_g1); *CXCL10* (Hs00171042_m1) *CD274* (Hs00204257_m1) and *RSAD2* (Hs00369813_m1) for qRT-PCR experiments. To confirm the use of equal amounts of RNA in each reaction, all samples were examined in parallel for beta-actin (Hs01060665_g1). Patient enrollment for these studies was done in collaboration with the Urology Service of the Vall d'Hebron Hospital. The study was approved by the Review Board of the Vall d'Hebron Hospital and informed consent was obtained from all patients before surgery (Ethics Committee reference: 00003437).

Ingenuity pathway analysis (IPA). Ingenuity Pathway Analysis (IPA) to study the microarray data was conducted using the Qiagen software (<https://digitalinsights.qiagen.com/>). In our study, IPA was used to detect and overlap the most significant regulated genes across different time and sex comparisons. A distinct data-filtering criterion was set: a log fold change cut-off of ± 0.5 . An individual analysis was performed for each comparison and the top 10 genes up- and down-regulated were reported. Their expression was represented in heatmaps.

Gene set enrichment analysis (GSEA) based pathway enrichment analysis. Pathway enrichment analysis was carried out by searching for enriched gene sets (e.g. pathways, molecular functional categories, complexes) for the different microarray comparisons using GSEA as previously described⁶² and depicted in Figure Supp3. The pathway gene set definition (GMT) files loaded on the software were created with the archived instance of g:Profiler (Ensembl 93, Ensembl Genomes 40 (rev 1760, build date 2018-10-02) with a *p* value cutoff: 0.01 for the microarray files. We used “gene set permutation” with 200 permutations to compute *p* values for enriched gene-sets, followed by GSEA's standard multiple testing correction.

Enrichment map pathway analysis visualization. The resulting enrichment results were visualized with the Enrichment Map plugin for the Cytoscape network visualization and analysis software. We loaded GSEA individual dataset using an FDR threshold between 0.01 and 0.1. A multi-dataset enrichment map comprising all comparisons was created with an FDR of 0.25. In the enrichment maps, each gene set is symbolized by a node in the network. Node size corresponds to the number of genes comprising the gene-set. The enrichment scores for the gene-set are represented by the node's color (red indicates up-regulation, blue represents down-regulation). To identify redundancies between gene sets, the nodes are connected with edges if their contents overlap by more than 50%. The thickness of the edge corresponds to the size of the overlap. The 3.7.1 Cytoscape version⁶³ was used with the following apps: EnrichmentMap^{62,64}, clusterMaker2⁶⁵, WordCloud⁶⁶, NetworkAnalyzer⁶⁷ and AutoAnnotate⁶⁸. Pathways are shown as circles (nodes) that are connected with lines (edges) if the pathways share many genes. Nodes are colored by ES, blue and red meaning down and up-regulated pathways, respectively. Edges are sized on the basis of the number of genes shared by the connected pathways. Network layout and clustering algorithms automatically group similar pathways into major biological themes. The EnrichmentMap software takes as input a text file containing pathway enrichment analysis results and another text file containing the pathway gene sets used in the original enrichment analysis. Gene sets were also visualized by heatmaps using online Heatmapper tool⁶⁹.

Statistics. Results were expressed as the mean \pm standard error of the mean (SEM). Student's t-test (two-tailed) was used for statistical analysis. A *P* value of less than 0.05 was considered to indicate statistically-significant differences. Statistical analyses were made with commercially available software (GraphPad Prism, version 6.00 for Windows, GraphPad Software, La Jolla California USA). Bioinformatic Analysis was performed using the free R and Bioinformatic software.

Received: 24 November 2021; Accepted: 30 March 2022

Published online: 28 April 2022

References

- Bellomo, R., Kellum, J. A. & Ronco, C. Acute kidney injury. *Lancet* **380**(9843), 756–766 (2012).
- Lameire, N., Van Biesen, W. & Vanholder, R. The changing epidemiology of acute renal failure. *Nat. Clin. Pract. Nephrol.* **2**(7), 364–377 (2006).
- Bonventre, J. V. & Yang, L. Cellular pathophysiology of ischemic acute kidney injury. *J. Clin. Investig.* **121**(11), 4210–4221 (2011).
- Chawla, L. S., Eggers, P. W., Star, R. A. & Kimmel, P. L. Acute kidney injury and chronic kidney disease as interconnected syndromes. *N. Engl. J. Med.* **371**(1), 58–66 (2014).
- Coca, S. G., Singanamala, S. & Parikh, C. R. Chronic kidney disease after acute kidney injury: A systematic review and meta-analysis. *Kidney Int.* **81**(5), 442–448 (2012).
- Hobson, C. E. *et al.* Acute kidney injury is associated with increased long-term mortality after cardiothoracic surgery. *Circulation* **119**(18), 2444–2453 (2009).
- Martin-Sanchez, D. *et al.* Targeting of regulated necrosis in kidney disease. *Nefrologia* **38**(2), 125–135 (2018).
- Rifkin, D. E., Coca, S. G. & Kalantar-Zadeh, K. Does AKI truly lead to CKD?. *J. Am. Soc. Nephrol.* **23**(6), 979–984 (2012).
- Ferenbach, D. A. & Bonventre, J. V. Mechanisms of maladaptive repair after AKI leading to accelerated kidney ageing and CKD. *Nat. Rev. Nephrol.* **11**(5), 264–276 (2015).
- Sanz, A. B., Santamaria, B., Ruiz-Ortega, M., Egido, J. & Ortiz, A. Mechanisms of renal apoptosis in health and disease. *J. Am. Soc. Nephrol.* **19**(9), 1634–1642 (2008).
- Ashkenazi, A. & Dixit, V. M. Death receptors: Signaling and modulation. *Science* (80-) **281**(5381), 1305–1308 (1998).
- Collins, A. J., Foley, R. N., Gilbertson, D. T. & Chen, S. C. United States Renal Data System public health surveillance of chronic kidney disease and end-stage renal disease. *Kidney Int. Suppl.* **5**(1), 2–7 (2015).

13. Mehta, R. L., Pascual, M. T., Gruta, C. G., Zhuang, S. & Chertow, G. M. Refining predictive models in critically ill patients with acute renal failure. *J. Am. Soc. Nephrol.* **13**(5), 1350–1357 (2002).
14. Paganini, E. P., Halstenberg, W. K. & Goormastic, M. Risk modeling in acute renal failure requiring dialysis: The introduction of a new model. *Clin. Nephrol.* **46**(3), 206–211 (1996).
15. Chertow, G. M. *et al.* Predictors of mortality and the provision of dialysis in patients with acute tubular necrosis. The Auriculin Anaritide Acute Renal Failure Study Group. *J. Am. Soc. Nephrol.* **9**(4), 692–698 (1998).
16. Wei, Q., Wang, M. H. & Dong, Z. Differential gender differences in ischemic and nephrotoxic acute renal failure. *Am. J. Nephrol.* **25**(5), 491–499 (2005).
17. Müller, V. *et al.* Sexual dimorphism in renal ischemia-reperfusion injury in rats: Possible role of endothelin. *Kidney Int.* **62**(4), 1364–1371 (2002).
18. Park, K. M., Kim, J. I., Ahn, Y., Bonventre, A. J. & Bonventre, J. V. Testosterone is responsible for enhanced susceptibility of males to ischemic renal injury. *J. Biol. Chem.* **279**(50), 52282–52292 (2004).
19. Jea, W., Hg, H. & Joeekes, A. M. REgional renal hypothermia. *Br. J. Urol.* **39**(6), 727–743 (1967).
20. Stueber, P., Kovacs, S., Koletsy, S. & Persky, L. Regional hypothermia in acute renal ischemia. *J. Urol.* **79**(5), 793–800 (1958).
21. Darius, T. *et al.* The effect on early renal function of various dynamic preservation strategies in a preclinical pig ischemia-reperfusion autotransplant model. *Am. J. Transplant* **19**(3), 752–762 (2019).
22. Hoyer, D. P. *et al.* Influence of oxygen concentration during hypothermic machine perfusion on porcine kidneys from donation after circulatory death. *Transplantation* **98**(9), 944–950 (2014).
23. Kathis, J. M. *et al.* Continuous normothermic ex vivo kidney perfusion improves graft function in donation after circulatory death pig kidney transplantation. *Transplantation* **101**(4), 754–763 (2017).
24. Hosgood, S. A. *et al.* A pilot study assessing the feasibility of a short period of normothermic preservation in an experimental model of non heart beating donor kidneys. *J. Surg. Res.* **171**(1), 283–290 (2011).
25. Rosen, S. & Stillman, I. E. Acute tubular necrosis is a syndrome of physiologic and pathologic dissociation. *J. Am. Soc. Nephrol.* **19**(5), 871–875 (2008).
26. Heyman, S. N., Rosenberger, C. & Rosen, S. Experimental ischemia-reperfusion: Biases and myths the proximal vs. distal hypoxic tubular injury debate revisited. *Kidney Int.* **77**(1), 9–16 (2010).
27. Heyman, S. N., Rosenberger, C. & Rosen, S. Acute kidney injury: Lessons from experimental models. *Contrib. Nephrol.* **169**, 286–296 (2011).
28. Khalid, U. *et al.* Kidney ischaemia reperfusion injury in the rat: the EGTI scoring system as a valid and reliable tool for histological assessment. *J. Histol. Histopathol.* **3**(1), 1 (2016).
29. Kanagasundaram, N. S. Pathophysiology of ischaemic acute kidney injury. *Ann. Clin. Biochem.* **52**(2), 193–205 (2015).
30. Gardner, D. S. *et al.* Remote effects of acute kidney injury in a porcine model. *Am. J. Physiol. Ren. Physiol.* **310**, 259–271 (2016).
31. Hannedouche, T. *et al.* Factors affecting progression in advanced chronic renal failure. *Clin. Nephrol.* **39**(6), 312–320 (1993).
32. Hauet, T. *et al.* Contribution of large pig for renal ischemia-reperfusion and transplantation studies: The preclinical model. *J. Biomed. Biotechnol.* **2011**, 532127 (2011).
33. Schook, L. B. *et al.* Swine Genome Sequencing Consortium (SGSC): A strategic roadmap for sequencing the pig genome. *Comp. Funct. Genom.* **6**, 251–255 (2005).
34. Huang, J., Bayliss, G. & Zhuang, S. Porcine models of acute kidney injury. *Am. J. Physiol. Ren. Physiol.* **320**(6), F1030–F1044 (2021).
35. Packialakshmi, B., Stewart, I. J., Burmeister, D. M., Chung, K. K. & Zhou, X. Large animal models for translational research in acute kidney injury. *Ren. Fail.* **42**(1), 1042 (2020).
36. Hannon, J. P., Bossone, C. A. & Wade, C. E. Normal physiological values for conscious pigs used in biomedical research. *Lab. Anim. Sci.* **40**(3), 293–298 (1990).
37. Capone, L., Marchetti, P., Ascierio, P. A., Malorni, W. & Gabriele, L. Sexual dimorphism of immune responses: A new perspective in cancer immunotherapy. *Front. Immunol.* **9**, 552 (2018).
38. Hosszu, A., Fekete, A. & Szabo, A. J. Sex differences in renal ischemia-reperfusion injury. *Am. J. Physiol. Ren. Physiol.* **319**(2), F149–F154 (2020).
39. Stambergova, H., Skarydova, L., Dunford, J. E. & Wsol, V. Biochemical properties of human dehydrogenase/reductase (SDR family) member 7. *Chem. Biol. Interact.* **207**(1), 52–57 (2014).
40. Beaudoin, J. J., Brouwer, K. L. R. & Malinen, M. M. Novel insights into the organic solute transporter alpha/beta, OSTa/b: From the bench to the bedside. *Pharmacol. Ther.* **211**, 107542 (2020).
41. Vorup-Jensen, T., Jensenius, J. C. & Thiel, S. MASP-2, the C3 convertase generating protease of the MBLectin complement activating pathway. *Immunobiology* **199**(2), 348–357 (1998).
42. Colvin, R. A., Campanella, G. S. V., Sun, J. & Luster, A. D. Intracellular domains of CXCR3 that mediate CXCL9, CXCL10, and CXCL11 function. *J. Biol. Chem.* **279**(29), 30219–30227 (2004).
43. Hoerning, A. *et al.* Peripherally circulating CD4 +FOXP3 +CXCR3 + T regulatory cells correlate with renal allograft function. *Scand. J. Immunol.* **76**(3), 320–328 (2012).
44. Naem, A. A., Abdulsamad, S. A., Rudland, P. S., Malki, M. I. & Ke, Y. Fatty acid-binding protein 5 (FABP5)-related signal transduction pathway in castration-resistant prostate cancer cells: a potential therapeutic target. *Precis. Clin. Med.* **2**(3), 192–196 (2019).
45. Asirvatham, A. J., Schmidt, M., Gao, B. & Chaudhary, J. Androgens regulate the immune/inflammatory response and cell survival pathways in rat ventral prostate epithelial cells. *Endocrinology* **147**(1), 257–271 (2006).
46. Francisco, L. M., Sage, P. T. & Sharpe, A. H. The PD-1 pathway in tolerance and autoimmunity. *Immunol. Rev.* **236**(1), 219–242 (2010).
47. Riella, L. V., Paterson, A. M., Sharpe, A. H. & Chandraker, A. Role of the PD-1 pathway in the immune response. *Am. J. Transplant.* **12**(10), 2575–2587 (2012).
48. Priante, G., Ganesello, L., Ceol, M., Del Prete, D. & Anglani, F. Cell death in the kidney. *Int. J. Mol. Sci.* **20**(14), 3598 (2019).
49. Elmore, S. Apoptosis: A review of programmed cell death. *Toxicol. Pathol.* **35**(4), 495–516 (2007).
50. Vendola, K., Zhou, J., Wang, J. & Bondy, C. A. Androgens promote insulin-like growth factor-I and insulin-like growth factor-I receptor gene expression in the primate ovary. *Hum. Reprod.* **14**(9), 2328–2332 (1999).
51. Nguyen, T. V., Jayaraman, A., Quaglino, A. & Pike, C. J. Androgens selectively protect against apoptosis in hippocampal neurones. *J. Neuroendocrinol.* **22**(9), 1013–1022 (2010).
52. Lin, Y. *et al.* Androgen and its receptor promote Bax-mediated apoptosis. *Mol. Cell. Biol.* **26**(5), 1908–1916 (2006).
53. Land, W. G. The role of damage-associated molecular patterns (DAMPs) in human diseases part II: DAMPs as diagnostics, prognostics and therapeutics in clinical medicine. *Sultan Qaboos Univ. Med. J.* **15**(2), e157–e170 (2015).
54. Yang, J. & Liu, Y. Dissection of key events in tubular epithelial to myofibroblast transition and its implications in renal interstitial fibrosis. *Am. J. Pathol.* **159**(4), 1465–1475 (2001).
55. Terada, Y. *et al.* Expression and function of the developmental gene Wnt-4 during experimental acute renal failure in rats. *Am. Soc. Nephrol.* **14**(5), 1223–1233 (2003).
56. Marino, L. & Colvin, C. M. Thinking Pigs: A Comparative Review of Cognition, Emotion, and Personality in *Sus domesticus*. *Int. J. Comp. Psychol.* <https://doi.org/10.46867/ijcp.2015.28.00.04> (2015).
57. Edgar, R., Domrachev, M. & Lash, A. E. Gene Expression Omnibus: NCBI gene expression and hybridization array data repository. *Nucleic Acids Res.* **30**(1), 207–210 (2002).

58. Barrett, T. *et al.* NCBI GEO: Archive for functional genomics data sets - Update. *Nucleic Acids Res.* **41**(D1), D991–D995 (2013).
59. Irizarry, R. A. *et al.* Exploration, normalization, and summaries of high density oligonucleotide array probe level data. *Biostatistics* **4**(2), 249–264 (2003).
60. Smyth, G. K. Linear models and empirical bayes methods for assessing differential expression in microarray experiments. *Stat. Appl. Genet. Mol. Biol.* **3**(1), 25 (2004).
61. Benjamini, Y. & Hochberg, Y. Benjamini-1995.pdf. *J. R. Stat. Soc. B* **57**(1), 289–300 (1995).
62. Reimand, J. *et al.* Pathway enrichment analysis and visualization of omics data using g:Profiler, GSEA, Cytoscape and Enrichment-Map. *Nat. Protoc.* **14**(2), 482–517 (2019).
63. Shannon, P. *et al.* Cytoscape: A software Environment for integrated models of biomolecular interaction networks. *Genome Res.* **13**(11), 2498–2504 (2003).
64. Merico, D., Isserlin, R., Stueker, O., Emili, A. & Bader, G. D. Enrichment map: A network-based method for gene-set enrichment visualization and interpretation. *PLoS ONE* **5**(11), e13984 (2010).
65. Morris, J. H. *et al.* ClusterMaker: A multi-algorithm clustering plugin for Cytoscape. *BMC Bioinform.* <https://doi.org/10.1186/1471-2105-12-436> (2011).
66. Oesper, L., Merico, D., Isserlin, R. & Bader, G. D. WordCloud: A Cytoscape plugin to create a visual semantic summary of networks. *Source Code Biol. Med.* **6**, 1–4 (2011).
67. Assenov, Y., Ramírez, F., Schelhorn, S.-E., Lengauer, T. & Albrecht, M. Computing topological parameters of biological networks. *Bioinform. Appl.* **24**(2), 282–284 (2008).
68. Kucera, M., Isserlin, R., Arkhangorodsky, A. & Bader, G. D. AutoAnnotate: A Cytoscape app for summarizing networks with semantic annotations. *F1000Res* **5**, 1717 (2016).
69. Babicki, S. *et al.* Heatmapper: Web-enabled heat mapping for all. *Nucleic Acids Res.* **44**, 147–153 (2016).

Acknowledgements

We thank all members of the Renal Physiopathology Group for valuable discussions. DNA microarray and the bioinformatics analysis were carried out by the Statistics and Bioinformatics Unit (UEB) of the Vall d’Hebron Research Institute (VHIR). This work reflects only the authors’ views, and the EU Community is not liable for any use that may be made of the information contained therein.

Author contributions

S.N., L.C., A.M., and J.M. contributed to conception and experimental design; L.C. performed IRI surgeries; S.N., L.C., D.R., M.E.S., M.A., A.S., M.F., J.M. and A.M. performed data acquisition or data analysis; and S.N., G.C.R. and A.M. prepared the manuscript, incorporating comments from other authors.

Funding

This work was supported in part by grants from Ministerio de Economía y Competitividad (SAF2014- 59945-R and SAF2017-89989-R to A. Meseguer), Red de Investigación Renal (REDinREN) (12/0021/0013 to A. Meseguer). Meseguer’s research group holds the Quality Mention from the Generalitat de Catalunya since 2005.

Competing interests

The authors declare no competing interests.

Additional information

Supplementary Information The online version contains supplementary material available at <https://doi.org/10.1038/s41598-022-10352-3>.

Correspondence and requests for materials should be addressed to A.M.

Reprints and permissions information is available at www.nature.com/reprints.

Publisher’s note Springer Nature remains neutral with regard to jurisdictional claims in published maps and institutional affiliations.



Open Access This article is licensed under a Creative Commons Attribution 4.0 International License, which permits use, sharing, adaptation, distribution and reproduction in any medium or format, as long as you give appropriate credit to the original author(s) and the source, provide a link to the Creative Commons licence, and indicate if changes were made. The images or other third party material in this article are included in the article’s Creative Commons licence, unless indicated otherwise in a credit line to the material. If material is not included in the article’s Creative Commons licence and your intended use is not permitted by statutory regulation or exceeds the permitted use, you will need to obtain permission directly from the copyright holder. To view a copy of this licence, visit <http://creativecommons.org/licenses/by/4.0/>.

© The Author(s) 2022